

CRR  
93/1996



HSE CONTRACT RESEARCH REPORT No. 93/1996

**MODELLING OF EXPLOSIONS AND DEFLAGRATIONS**

---

***P W Guilbert and I P Jones***

---

Computational Fluid Dynamics Services  
Building 8.19  
Harwell Laboratory  
Oxfordshire  
OX11 0RA

---

NOT TO BE  
TAKEN AWAY

FOR  
REFERENCE ONLY



---

HSE CONTRACT RESEARCH REPORT No. 93/1996

## MODELLING OF EXPLOSIONS AND DEFLAGRATIONS

---

*P W Guilbert and I P Jones*

---

Computational Fluid Dynamics Services  
Building 8.19  
Harwell Laboratory  
Oxfordshire  
OX11 0RA

---

St Paul City  
Pub'd  
7-2-96

It is well known that premixed gas-air and dust-air mixtures can be highly explosive if significant amounts of turbulence are present or are generated as burning occurs. Flame speeds which may only be a few metres per second in laminar conditions can rise to hundreds of metres per second if turbulence is present. This project was primarily directed at producing a tool to investigate such explosions in uncongested systems of moderate dimensions such as flame proof enclosures. A rather simplified model of dust explosions was also implemented which was designed to simulate the worst case, of premixed, fine dust and air mixtures. In addition to the modelling it is also important to have good software for interpreting the results of simulations as a very great deal of data is produced. To deal with this a specialised graphical visualisation package was produced to allow detailed three dimensional graphics, both static and animated. This proved to be of great value in interpreting the results and comparing with high speed videos of the experiments conducted at HSE.

This report and the work it describes were funded by the Health and Safety Executive. Its contents, including any opinions and/or conclusions expressed, are those of the authors alone and do not necessarily reflect HSE policy.

© Crown copyright 1996

Applications for reproduction should be made to HMSO

First published 1996

ISBN 0 7176 1035 7

All rights reserved. No part of this publication may be reproduced, stored in a retrieval system, or transmitted in any form or by means, electronic, mechanical, photocopying, recording, or otherwise, without the prior written permission of the copyright owner.

# CONTENTS

1	INTRODUCTION.	1
2	PROGRAMME OF WORK.	1
	2.1 ENVIRONMENT 1.5a.	1
	2.2 SOPHIA, setting up the geometry.	1
	2.3 CFDS-FLOW3D.	2
	2.4 Visualisation of results.	2
	2.5 Dust explosion modelling.	2
	2.6 Gas explosion modelling.	3
	2.7 Applications.	3
	2.8 Documentation and software.	3
	2.9 Budget.	3
	2.10 Reports.	3
3	RECAP OF PHASES ONE AND TWO.	3
	3.1 Phase 1.	4
	3.2 Phase 2.	4
4	GAS EXPLOSION MODELLING.	5
	4.1 Ignition.	5
	4.2 Thin flame stage.	6
	4.3 The highly turbulent deflagration stage.	6
	4.4 Turbulent quenching.	6
	4.5 Vent model.	6
	4.6 Rough wall effects.	6
5	DUST EXPLOSION MODELLING.	7
6	SOFTWARE DEVELOPMENT.	7
	6.1 Physical models.	8
	6.2 Numerics.	9
	6.3 Flame front tracking.	9
	6.4 Data Base.	9
	6.5 Three dimensional animation output.	10
7	APPLICATIONS.	10
	7.1 Linked vessels.	10
	7.2 The HSE baffled enclosure experiments.	11
	7.3 The HSE vented, baffled box experiments.	12
	7.4 The CCRL furnace case.	13
	7.5 The Peat bomb experiments.	14
	7.6 Miscellaneous cases.	15
8	CONCLUSIONS.	15

8.1	Phase three.	15
8.2	The explosion modelling project.	16
8.3	Possible future developments.	16
9	REFERENCES.	18

### Figures

Figure 1.	Methane-air, vessel one.	19
Figure 2.	Methane-air, vessel two.	20
Figure 3.	Central ignition, methane-air.	21
Figure 4.	Central ignition, methane-air.	22
Figure 5.	End ignition, methane-air.	23
Figure 6.	Explosion in a closed baffled box.	24
Figure 7.	Baffled box, methane-air.	25
Figure 8.	Baffled box, methane.	26
Figure 9.	Peat dust bomb.	27

### Appendices

Appendix 1	The Ignition Model.	28
Appendix 2	The thin flame model.	30
Appendix 3	The Eddy Break Up combustion model.	32
Appendix 4	Quenching.	34
Appendix 5	Dust combustion model.	35
	1 INTRODUCTION.	35
	2 TRANSPORT OF GAS AND DUST FRACTIONS.	35
	3 EQUATION OF STATE.	36
	4 RADIATION TRANSFER.	37
Appendix 6	Three dimensional animations.	39

## **EXECUTIVE SUMMARY.**

### **Modelling of Explosions and Deflagrations.**

This report describes the work done by the CFDS department of AEA Technology on behalf of HSE for the modelling of explosions. The project lasted approximately three and a half years and was divided into three phases. A variety of tasks were performed as a part of the contract but the most important objectives were: to demonstrate a capability to simulate high speed reacting flows, and gaseous deflagrations in particular; to provide validated models of gas and dust deflagrations; and to provide customised software for HSE. These objectives have all been met and the software package has been delivered to HSE at Buxton and is now in use there.

It is well known that premixed gas-air and dust-air mixtures can be highly explosive if significant amounts of turbulence are present or are generated as burning occurs. Flame speeds which may only be a few metres per second in laminar conditions can rise to hundreds of metres per second if turbulence is present. This project was primarily directed at producing a tool to investigate such explosions in uncongested systems of moderate dimensions such as flame proof enclosures. A rather simplified model of dust explosions was also implemented which was designed to simulate the worst case, of premixed, fine dust and air mixtures. In addition to the modelling it is also important to have good software for interpreting the results of simulations as a very great deal of data is produced. To deal with this a specialised graphical visualisation package was produced to allow detailed three dimensional graphics, both static and animated. This proved to be of great value in interpreting the results and comparing with high speed videos of the experiments conducted at HSE.

All the modelling was performed using an adapted version of the CFDS-FLOW3D flow simulation program, a commercial software package. Additional software modules specific to the modelling of explosions have been supplied together with the modified code. These modules include: the implementation of an ignition model; a quasi-laminar flame transport model; flame quenching models and a modified version of the Eddy Break Up model for turbulent burning. Additionally for dust explosion modelling there are modules to allow for: modifications to the fluid equation of state due to the particles; devolatilisation of particles and radiative heat transfer. This software allows for modelling of a deflagration from the initial ignition in a quiescent fluid through to final burn out and represents the state of the art for its intended areas of application. The software has been applied to a number of systems for which experimental data are available. These include:-

- a shock tube, to test for the ability to model transonic flows;
- the Raufoss baffled tube experiment;
- the Leeds University linked vessels experiments;
- closed baffled boxes, representing flame proof enclosures;
- vented enclosures;
- a dust explosion in a spherical container.

The baffled box and vented enclosure experiments were all carried out at HSE, Buxton.

The conclusions of the work are as follows:-

- 1 The software delivered to HSE is capable of modelling a wide variety of explosions, both gas and dust.
- 2 The graphical package provides an advanced three dimensional visualisation capability essential for analysing the results, especially for large three dimensional simulations.
- 3 The experience gained on the application of the software demonstrates that, on the whole, agreement with experiment is encouraging and that modelling is an important tool in the field for the safety engineer.
- 4 The models are not yet ready to be used as a 'black box'. They do need some calibration of parameters which may be system dependent. Once a calibration has been performed, however, then predictions may be made for all systems which fall in the same class, i.e. which are of a similar scale and topology.
- 5 Because of the need for care in the application of CFD experiments are still needed to provide validation when a new class of systems is to be investigated.
- 6 As more and more classes of systems are investigated the methodology will improve as its range of validity is increased and greater confidence can be attached to the results.

## 1 INTRODUCTION.

This report describes the work done to complete Phase 3, the final phase, of the project to model explosions and deflagrations for HSE. In addition to a detailed discussion of the Phase 3 work a summary of all the work done over the entire project is provided as the project is now completed.

The main thrust of the Phase 3 work has been to improve the gaseous explosion models, particularly through the use of the HSE experiments on baffled boxes as validation cases. In addition to this, physical models for simple dust explosion simulations have been added and two validation cases have been completed. The user interface to the explosion models has been improved and extended so that no user Fortran is necessary to set up a standard model. For visualisation purposes a three dimensional animation package has been included, the graphics are generated using a customised version of the AVS software which has been included as an addition to the FLAVIA package.

## 2 PROGRAMME OF WORK.

This section summarises the work done to fulfil Phase three of the explosion modelling project.

### 2.1 ENVIRONMENT 1.5a.

This is the latest release of the CFDS fluid dynamics environment, HSE has already received a copy of this. SOPHIA, in particular, has been greatly improved and the extrusion facility makes the generation of pipes very easy. A new post-processor, FLAVIA, has been added to the ENVIRONMENT, and this provides considerably enhanced graphics for three dimensional models.

CFDS-FLOW3D now includes many of the algorithmic improvements needed for explosion modelling as standard, considerably reducing the amount of special Fortran needed to simulate explosions. This greatly eases the support needed for the explosion software and increases the fraction of the customised code which deals with the actual modelling.

### 2.2 SOPHIA, setting up the geometry.

HSE has an interest in simulating pipe networks and the ability of SOPHIA to support a library of geometrical groups, which can be used to build up geometries LEGO fashion, was to be used to provide the necessary building blocks for a network. This has been largely superseded by the new extrusion facility in SOPHIA. A right angled T-junction of equal diameter pipes has been generated and supplied to HSE. All the other components, e.g. straight lengths and bends, can be generated so quickly using face extrusion that a group library of such parts is redundant, and so it has not been supplied. It is worth noting here that the T-junction consists of about 40 blocks and pipes of 5 blocks each and so networks will consist of large numbers of blocks. This reduces the efficiency of CFDS-FLOW3D. FEF3D is a new program supplied with the ENVIRONMENT which is designed to be used to convert unstructured meshes to the blocked meshes used by CFDS-FLOW3D. In addition FEF3D can be used to reblock SOPHIA meshes. For pipe networks

where the blocks join onto one another in a simple fashion this can be expected to very greatly reduce the total number of blocks used, thus restoring the efficiency of CFDS-FLOW3D.

### 2.3 CFDS-FLOW3D.

The command language has been extended to allow for simplified setting up of gas explosion models and also for setting up dust explosion models. New fuel component types have been added to the combustion model, water and ethylene, and the code which sets up the fuel has been greatly simplified so that a new fuel component can be easily added by simply entering the data for it in a single routine.

A two Damköhler number model for the quenching has been added, otherwise the gaseous combustion model is unchanged.

The dust explosion model is a generalisation of the eddy break up combustion model used for gaseous explosions. A great deal of new code has been added for this to model the particle vaporisation and the heat transport due to radiation. In addition the equation of state needed to be modified. The Fortran used to model the chemical igniter in the dust explosion used for validation, see below, has been left as a template.

Flame front tracking and automatic convergence control have been standardised but the coding still occurs in user routines so that HSE have easy access to this code, e.g. should the convergence control prove inadequate.

New three dimensional animation software has been added. This directly replaces the two dimensional code and uses the same command language.

Two major requirements of the contract, a physical data base and a rough wall treatment, have been supplied as standard developments. For gaseous explosion modelling, however, the simplification in adding new fuel types is probably as important, if not more so, than the data base.

### 2.4 Visualisation of results.

The new AVS based visualisation program, FLAVIA, has been supplied as a part of the contract. In addition a specially customised version of the AVS software has been put together to allow for three dimensional animations to be produced. This consists of two parts: the first is used to create the pictures used in the animation from the data files supplied by CFDS-FLOW3D, and the second is used to play back these pictures to produce the animation.

### 2.5 Dust explosion modelling.

A simple model for premixed dust air mixtures has been implemented. Two validation cases have been simulated to test the software and the models. One case was not an explosion but a steady state coal furnace calculation. This calculation was performed simply to test the physical models used for devolatilisation and radiation in a limit where they should give a good comparison with the standard particle models used in CFDS-FLOW3D and the radiation models in RAD3D. A small scale experiment, of a peat dust bomb, used

by Kjaldman, see below, was used for direct validation of the models. A paucity of appropriate experiments has prevented further validation and so no further simulations have been performed for dust.

## 2.6 Gas explosion modelling.

Quenching of the flame in the laminar and turbulent phases has been improved by using a separate Damköhler number for each. This has been validated using the Leeds linked vessel experiment, Phylaktou and Andrews, 1993.

Unvalidated additions to the turbulence model have also been supplied to HSE. These additions are two extra terms which allow for pressure-strain correlations not included in the standard K-epsilon model. One of the terms includes the generation of turbulence through Rayleigh-Taylor instability at the flame front and so is a potentially important source of non-shear generated turbulence.

## 2.7 Applications.

The Leeds linked vessel experiment, Phylaktou and Andrews, 1993, has been simulated for both the central and end ignition cases. The centrally ignited enclosed baffled box experiment performed at HSE, Buxton, has been simulated. The open ended baffled box has received the most attention with many simulations attempted. A 20 litre peat dust bomb, as detailed by Kjaldman, 1992, has also been simulated. All the cases set up for simulation, including SOLVEX and the Raufoss tube have been supplied to HSE.

## 2.8 Documentation and software.

All the software, setup files for application examples, example animation files and the T-junction group file for SOPHIA have been supplied on tape to HSE, together with documentation. The Fortran has been supplied in both single and double precision.

## 2.9 Budget.

The work was carried out to budget. The timescale for the work was extended to the end of September 1994.

## 2.10 Reports.

Four quarterly progress reports and this document.

## 3 RECAP OF PHASES ONE AND TWO.

In order to give a complete picture of all the work done and the progress made over the entire project, a recap of phases one and two is given below. Only an overview is provided as details can be found in the reports provided during and at the end of each phase. At the end of each phase a complete set of software; the latest CFDS ENVIRONMENT plus all the developments during the project, Fortran source and files necessary to run validation examples, were delivered to HSE at Buxton. Additionally during Phase 2 a special set of software was provided for use on a 486 based PC running Microsoft Windows, DBOS and the DOS operating system.

### 3.1 Phase 1.

At the inception of this project CFDS-FLOW3D had not been used for modelling high speed reacting flows. The first and most important step was thus to demonstrate a capability to simulate such flows. Calculations were carried out for shock tubes and De Laval nozzles to demonstrate solutions for flows with supersonic speeds; a regime extending beyond that required for deflagrations where speeds are generally subsonic.

The Eddy Break Up (EBU) model for combustion was already available as a part of the standard software. The model was extended, in the same manner as had been done by Bakke (1986), to include an ignition/quenching mechanism based upon a Damköhler number. This number was computed from the ratio of the chemical to the turbulent eddy timescales; the chemical timescale itself was based upon a simple Arrhenius rate.

Most of the validation work was based on simulations of the large baffled cylinder experiments performed at Raufoss, Moen et al. (1982). Although these experiments were subsequently dropped for validation work, the attempts to simulate the methane-air case provided the experience which was the foundation of all future developments. By simply following the approach of Bakke (1986) similar, reasonable agreement with experiment was obtained. As soon as sensitivity analyses of the numerical results to variations in time stepping, grid resolution, differencing schemes etc. were performed it became clear that little confidence could be attached to the results. In addition it was obvious that models were needed for the pre-turbulent phase of the explosion and that the Damköhler number approach for ignition was inadequate.

An ability to model high speed reacting flows had been demonstrated.

### 3.2 Phase 2.

Most of the work in this phase was directed towards developing CFDS-FLOW3D into a robust, reliable and efficient program for modelling high speed reacting flows. Additionally, model development was required for a complete simulation of an explosion from ignition to burn out. Other tasks, such as a PC version of the software and a feasibility study for dust explosion simulation, were also carried out and these are detailed in the Phase 2 report.

New models were added to simulate: ignition; quasi-laminar flame front propagation and turbulent quenching. The Damköhler number based on an Arrhenius rate was dropped although this model remained in the standard software. The addition of these models enabled much greater accuracy in the estimation of the total duration of a deflagration, which is dominated by the slow burning pre-turbulent phase. Also, because the EBU model is only used for the high turbulence phase where it is applicable, no artificial initialisation of the turbulence field is needed and simulations of experiments with zero initial turbulence can be modelled directly. This removed the model sensitivity to initial conditions and so reliable results could be obtained.

CFDS-FLOW3D was mainly used for incompressible steady state simulations and so even though it was capable of accurately finding solutions for transient highly compressible flows it was neither efficient nor robust. In order to simulate an explosion it is necessary to perform hundreds or thousands of time steps with flow speeds changing from zero to hundreds of metres per second. Also, due to the combustion, gas temperatures may vary

by a thousand degrees over a few grid cells. Improvements to the numerical algorithms resulted in an order of magnitude improvement in the efficiency of the program and allowed complete simulations, from ignition to burn out, to be completed without any human intervention.

Numerical accuracy is essential for getting reliable solutions to the models. A new second order time differencing scheme was introduced which guaranteed positivity when necessary. This enabled second order differencing in both space and time to be used thus removing numerical diffusion, which is essential if accurate grid independent and time step independent solutions are to be produced with feasible spatial and temporal resolution. Other less vital improvements to accuracy were also introduced, see the Phase 2 report.

Once the software was capable of efficiently producing accurate model solutions validation was the most important requirement. Throughout this development phase the Leeds linked vessel experiments, Phylaktou, H and Andrews, G.E, (1993) were used for validation. These experiments had the major advantage of being well specified and, because there was no venting, no uncertainties due to fluid boundaries existed. The methane-air experiment with central ignition in one of the vessels tested both the models and the numerical algorithms very rigorously. The results were generally very good though the flame speed in the quasi-laminar phase was consistently underestimated.

Accurate, robust and efficient software for modelling a complete deflagration had been demonstrated. The models themselves had been validated.

#### 4 GAS EXPLOSION MODELLING.

During this phase of the project the gas explosion models did not change greatly. Some modifications were introduced, however, in order to improve the performance of the simulations in the pre-turbulent phase. In addition the quenching was modified to allow for different mechanisms to operate in the quasi-laminar and EBU phases. Note that the details of all the models used can be found in appendices one to four. Control of the models, setting up the fuel parameters, locating the ignition region and setting the model parameters has now all been included in the command language used to run CFDS-FLOW3D avoiding the necessity for the user to change any Fortran for different simulations. All the extra command language is documented in a file included with the software already delivered to HSE.

##### 4.1 Ignition.

The model assumes that the ignition region is traversed by a laminar flame which burns it out completely and so the ignition source term should peak just as the ignition region burns out and then cut-off immediately. Originally an exponential function with a time constant equal to the flame crossing time across the ignition region was used but this produced an unphysically extended ignition time and reduced the peak burning rate. The cut-off was modified to be a simple switch which turns off the ignition source term at a user specified number of flame crossing times across the ignition region. The exponential cut-off was used to provide a smooth transition into the quasi-laminar model, however, the non-smooth function now used does not appear to cause any additional difficulties. The

new function improves the timescale for the modelled ignition so that it is much closer to the actual timescale, removing errors as large as 10-20 milliseconds for cruder grids which have large ignition regions.

#### 4.2 Thin flame stage.

The laminar flame speed is no longer treated as constant, instead a simple parabolic function of the equivalence ratio is used. The treatment is the same as that used by Bakke, (1986). This enables inhomogeneous gas air mixtures to be simulated, e.g. the burning in a venting region. In addition the new quenching functions used, see below, require the correct laminar flame burning rate. From the user's point of view it also allows the specification of the laminar flame model to be set up much more easily, since no calculations of flame speed as a function of mixture have to be made.

#### 4.3 The highly turbulent deflagration stage.

The model for this is unchanged from Phase 2 except that a new quenching function is used, see below.

#### 4.4 Turbulent quenching.

The quenching model has been extended to allow for the different physical regime of burning when in the eddy break up phase as opposed to the thin flame phase. The previous model simply compared the laminar strain due to turbulence with the laminar burning rate. This is appropriate in the thin flame phase where the picture is one of stretched flamelets, however, it does not seem appropriate for the highly turbulent phase when the combustion takes place in the micro-scale eddies. For the high turbulence phase, therefore, the quenching is based on a comparison between the eddy dissipation rate and the laminar burning rate (which is proportional to the chemical rate). This is effectively a two Damköhler number model for the quenching. Testing on the Leeds linked vessel experiment indicates that this model performs considerably better than the old single Damköhler number model. See appendix 4 for details.

#### 4.5 Vent model.

A simple model of a vent has been implemented. In the case where a vent opens, or breaks, to allow sudden pressure relief simple flow resistances are introduced at the vent location. The resistance is high enough to reduce the flow to a negligible rate before the venting begins and is removed altogether when the over pressure reaches the relief value. This has been tested for the baffled box experiment at Buxton.

#### 4.6 Rough wall effects.

In all the work done for this project the walls of any vessel have been modelled as completely smooth. In many situations it is quite likely that walls will actually be rough, at least in a fluid dynamics sense. This is particularly important for modelling flame acceleration in systems where obstacles do not exist so that wall shear is the dominant source of turbulence generation, e.g. in long straight pipes. There is a new user routine included with the release of CFDS-FLOW3D which has a template calculation included for a completely rough wall. The only parameter which needs to be set is the roughness height.

## 5 DUST EXPLOSION MODELLING.

Dust explosions are considerably more complex than gas explosions due to the greater amount of physics involved. In the general case dust has to be lifted up into the air first to give an explosive mixture. Then the dust particles must be heated to release volatile gases which will burn. The physical processes happening at the particle surface and inside the particle as it is heated are complex and depend in detail on the particle composition and structure. In addition to the physical complexities of particle pyrolysis, particle dynamics must also be treated separately if the particles are large.

A dust explosion model has been implemented which is essentially a generalisation of the gaseous explosion model. Mathematical details can be found in appendix 5. The model for dust burning is a very simple one: the dust is assumed to be in dynamic and thermal equilibrium with the gas; all heterogeneous char combustion is ignored; all particle size effects in pyrolysis are ignored and the particles themselves are spherical and of fixed size; particle-particle interactions, e.g. agglomeration, are ignored; devolatilisation is assumed to proceed as a simple one step Arrhenius reaction and, finally, the standard gaseous combustion models used for deflagrations are assumed to apply to the gas phase combustion. In addition no modelling of the lifting off, or settling onto, surfaces of dust is included, that is the dust is assumed to be premixed.

Basically the picture is that all the solid phase fuel, held in the dust, is released, as radiative and convective heating causes devolatilisation through dust pyrolysis, and then it burns in the gaseous phase. Due to the simplifying assumptions made above the dust and gas can be treated as a single multi-component fluid and so the system can be approximated as a straight forward generalisation of the gaseous explosion model, see appendix 5.

A further complication arises in the case of dust, and that is radiative heat transport. In purely gaseous systems radiation can be ignored, to a good approximation, except in very large systems. For fine dusts, 100 micron diameters and less, in systems with dimensions of metres or more it is easy to show that radiation cannot be ignored. Such systems are optically thick to absorption by dust and so a simple radiation diffusion model has been included.

It is clear from all the assumptions made in order to provide a tractable model that this is not of general applicability. However, it is hoped that it does provide the worst case. In practice, with the exception of coal dust and a few other special materials, insufficient data exists to justify the use of a more complicated model. Even for this model the Arrhenius rate parameters for devolatilisation are needed and may well not be readily available. The experiments used by Kjaldman, (1992) for validating his model have been used here also because all the necessary data was available.

## 6 SOFTWARE DEVELOPMENT.

In order to simulate deflagrations the models described in sections 4 and 5, and in appendices 1 to 5, a special set of extra and modified routines have been implemented into CFDS-FLOW3D and supplied to HSE with documentation. So that the software can be used without specialised knowledge of its implementation the setting up of a simulation is now all provided for in the command language used to control CFDS-FLOW3D. Details

of the command language and examples of its use have been provided with the software. In addition to the models and the command language a variety of additional features have been added to improve the performance of the software, to enable new fuel types to be added much more easily, to allow flame tracking and to provide for full three dimensional animations.

## 6.1 Physical models.

Little change has been needed for the gas explosion models except that initialisation is now done through the CFDS-FLOW3D frontend with extended command language to allow complete problem specification without recourse to Fortran. In particular the ignition model has been removed from the user source specification subroutine and the location and duration of ignition is now set in command language. The ignition and quenching models have been modified as discussed in sections 4.1 and 4.4 above, and see appendices 1 and 4. A new fuel type ethene (ethylene) has been added and water can also be a fuel component. The specification of fuels for the EBU model has now been greatly simplified and provided the fuel is one of, or a mixture of, the hydrocarbon fuels provided as standard then all that is needed to specify the fuel is its composition.

In order to model dust explosions considerable additions had to be made. The dust is considered to consist of two components: an inert component which is simply conserved and takes no part in the combustion process and a component which on heating is converted into combustible gas. The components are referred to as dust inert and dust fuel, respectively. The standard EBU combustion model has been extended, therefore, to include two extra mass fractions, dust fuel and dust inert. Because radiation must also be considered an extra combustion scalar is included to represent the mean radiation intensity. Extra equations to represent the transport of dust fuel, dust inert and radiation have been added. Details of these equations can be found in appendix 5. The dust is treated as two extra components of the fluid and so the equation of state describing the fluid has had to be modified from that of a simple perfect gas. The dust particles are incompressible and act like molecules of infinite molecular weight, thus they contribute nothing to the bulk pressure and are included only as an extra source of inertia, reducing the speed of sound.

Radiation transport is modelled as a simple diffusion process. Recent modifications to the standard code allowing convection terms to be switched off made this much easier to implement. For technical reasons, however, boundary conditions had to be implemented specially as the radiation does not obey the same conditions as fluid at walls and fluid boundaries. The radiation boundary conditions were not implemented in the full generality available using RAD3D, in particular the radiation temperature is assumed to equal the wall temperature at walls and Neumann conditions are used at all fluid boundaries.

Dust explosions require a large ignition source to initiate them, unlike gas explosions. The simple point source ignition function used for gas explosions is thus inadequate for dust explosions and a model of a chemical igniter has been included using user Fortran. The location of the ignition can still be specified in command language but the igniter properties, mass injection rate, heat injection rate etc. have to be specified in the Fortran. A template calculation has been provided which models the chemical igniters used for the Kjaldman (1992) dust bomb experiments.

## 6.2 Numerics.

Only minor additions and improvements have been made in Phase 3. New TVD (Total Variance Diminishing) differencing schemes have been introduced, and, in addition, a modification to the QUICK scheme called CCCT has been implemented. These schemes, like CONDIF the scheme used for all the work done in this project, are bounded and second order and so avoid numerical diffusion and can be used for positive definite variables. The TVD schemes are often used in high speed flow calculations where they give much better resolution of shock fronts. Tests with the TVD schemes give results comparable with CONDIF but have proved more expensive to use due to having poorer convergence properties. A major concern with CONDIF is that it is not an exactly conservative scheme, however, in only one case has this ever proved to be significant causing a few per cent change in mixture fraction. Consequently due to its better convergence properties CONDIF is still the scheme of choice.

Improved mass conservation has been enforced for systems with no pressure boundaries. In particular non-ideal gas equations of state are supported and single precision can be used if preferred. The routines have also been updated to allow for mass sources.

The second order backward time differencing algorithm has been extended to allow for non-continuous mass sources. As implemented the algorithm did not conserve mass etc. if sources and sinks were switched on and off in one time step.

The main cause of a simulation failure is when simple time step adaption is insufficient to ensure solution convergence. In order to improve the robustness of the software automatic convergence control has been introduced. This is based on heuristics garnered from experience with obtaining convergence manually and is not guaranteed to work in every case. When this facility is used all user settings of under relaxation factors are ignored.

## 6.3 Flame front tracking.

In cases where the flame front does not move through the same region of space more than once the time of arrival of the flame is a single valued function of position. For such flames it is possible to display the flame kinematics graphically without using animation. The arrival time of the flame is stored as a scalar field and an isosurface of this variable, an isochrone, is coincident with the flame front at the time represented by the isosurface. For kinematic visualisation the AVS visualisation software supplied to HSE, HSE1VIEW, has a facility for displaying isosurfaces and running through a sequence of different values automatically. This enables the development of the flame front in time to be observed without animation.

## 6.4 Data Base.

Physical data base software is now included and access is provided to the PCP, DIPPR and INFOCHEM data bases. Also user data bases can be set up. In practice for explosion modelling, however, these developments have been superseded by considerable improvements to the combustion frontend in CFDS-FLOW3D. The specification of a fuel is now made by simply naming each of the fuel components, e.g. methane, ethane etc., and specifying the fractional composition in terms of each of these components. The software has

also been modified so that adding a new fuel type is simply a question of specifying its properties, heat of reaction, molecular weight and so forth, in a single routine. It then immediately becomes available for use as a legal fuel component type in the command language.

### 6.5 Three dimensional animation output.

In principle 3 dimensional animations could be generated by simply writing out all the variables, or just those required, to the dump file every time step or every predetermined amount of model time. This approach would generate enormous dump files, however, and so a special set of files containing just the data required is printed out. For standard two dimensional animations where data is written out for planes there is one file per plane containing dumps of the variables wanted. Because of the extra data involved in a full 3 dimensional animation the dumps are each written to a separate file. For example if a dump was to be made every millisecond of model time for ten milliseconds then ten files would be created. In order to reduce the size of these files even further only changes in variable values are stored and only those changes which are significant, see appendix 6 for full details. In explosion modelling most of the changes occur at the flame front and so a great deal of data can be saved by this method. Control of the output is effected using the same command language that the two dimensional animation uses. Two and three dimensional animations cannot, therefore be created simultaneously.

## 7 APPLICATIONS.

Most of the work on experimental validation has again used the Linked vessel data from Leeds, Phylaktou and Andrews, (1993). A great deal of work has also been done in collaboration with HSE on the experimental work there using a closed box with internal baffles and a vented box also with baffles. For validation of the dust explosion model two cases were investigated: the spherical peat dust bomb, Kjaldman, (1992) and a steady state calculation of coal combustion in the CCRL furnace, Sykes, (1990). The CCRL furnace calculation is not an explosion simulation but was used to validate the physical models for devolatilisation and radiation against the standard models for coal combustion in the software.

### 7.1 Linked vessels.

Experimental data available for this case are excellent and the geometry generates extremely high flame speeds and pressure rises. Also because the system is closed, no gas can escape, the pressure rise is a measure of the combustion rate as well as the combustion dynamics. In Phase 2 a great many partial simulations of the central ignition case were performed to shake down and validate all the additions to the software, both the physical and the numerical models. In this phase the central ignition case has been used to calibrate the new quenching model. The end ignition case has been used as a validation case.

The apparatus consists of two cylinders of 0.5 m diameter and 0.5 m length connected at their axis by a pipe of 76 mm diameter and 1.7 m long. For the experiments which have been simulated the apparatus is initially filled with a ten per cent methane air mixture,

approximately stoichiometric, and is ignited either at a point in the centre of one of the vessels or at the closed end. The details of the experimental set up and the results are discussed at length by Phylaktou and Andrews, (1993).

In the central ignition case the flame grows slowly for the first 50 ms or so when it reaches the connecting pipe. Then it accelerates and travels the length of the pipe in a little over 10 ms. Flame speeds in the pipe rise to about  $130 \text{ ms}^{-1}$ . When the flame exits the pipe into the second vessel flame speeds increase to  $370 \text{ ms}^{-1}$  causing a very violent explosion. The burning rate in the first vessel then increased dramatically also. This case was used to calibrate the quenching and the laminar flame model. Comparisons between simulation and experiment for the pressure rises in the two vessels are given in figures 1 and 2. Figures 3 and 4 show the pressure histories for the two vessels plotted on the same graph for experiment and simulation, respectively.

In the end ignition case the flame takes about 100 ms to reach the connecting pipe and only 7 ms to 8 ms to travel through the pipe. In this case the explosion in the second vessel is very violent indeed. For central ignition the peak rate of pressure rise in vessel two is 548 bar per second; in the end ignition case the peak rate is 2068 bar per second. The results of the simulation can be seen in figure 5. The simulation gives a flame arrival time at the pipe of 105 ms and a flame travel time through the pipe of 4 ms.

In both cases the quasi-laminar flame stage is well simulated but the pressure rise after the flame ignites the second vessel is slower. This is due to the quenching used. If the quenching is reduced then the flame travel time through the pipe is too small. Even with the current quenching it is too small in the end ignition case. It is probable that the quenching model is too simple as it takes no account of the dependence of laminar flame speed on temperature and pressure. In vented examples where pre-compression and heating are not so significant the model performs better. Not only is the unburnt gas precompressed but gas exits from the connecting pipe with a velocity which may exceed the speed of sound in the cold gas and so the combustion process is moving into a regime far removed from the original EBU concept. It is perhaps not surprising that modelling deficiencies have begun to show up here.

## 7.2 The HSE baffled enclosure experiments.

HSE at Buxton conducted a series of experiments in a closed box of dimensions 586mm by 494mm by 340mm. Inside the box is a base plate from which a number of baffles can be hung. Details of the experiments can be found in the HSE internal report by Allsop, J.A. and Eaton, G.E., (1994). Results for the methane and propane simulations for central ignition behind the base plate are shown in figure 6. These simulations are fully three dimensional and demonstrate, for the first time, the ability of the software to cope with a geometrically complex situation.

The agreement between simulation and experiment is quite good, however, the peak pressure achieved in the simulations is about 1.5 bar too high. Isothermal wall boundary conditions were used so the model had the maximum possible heat loss to the walls. An extended run for the propane case gave a cooling time of the order of 10 seconds, where as the experimental results indicated a cooling time of the order of 1 second. Even though the time to peak pressure is 0.2 seconds or less it is clear that cooling is important. Radiative cooling which has been ignored will make at most a ten percent difference to the peak

pressure, too little to explain the discrepancy. In the simulations the walls in the vessel were assumed to be smooth from a fluid dynamic point of view, inspection of the inside of the box and of the baffle plates actually shows considerable pitting giving a roughness height of the order of millimetres. This is sufficient to considerably enhance the heat transfer rate to the wall. It is most likely that this is the explanation for the peak pressure discrepancy since the surface area of the box walls plus baffles is quite large.

### 7.3 The HSE vented, baffled box experiments.

These experiments have been extensively investigated. The experiment consists of box with internal dimensions of 1200mm by 300mm by 300mm with a number of equally spaced baffles bolted to both sides of the box. The full details can be found in the HSE internal report by Freeman, D.J., (1994). The only experiment which has been simulated is the case with five equally spaced baffles of width 75mm with a 10% methane air mixture. The experiment showed peak pressures of about 1 bar for this case. A great many simulations were carried out, however, peak pressures of only about 0.2 bar could be achieved.

The results of the simulations for this case were rather disappointing and so a great deal of effort has been directed to investigating the causes for the failure since it would seem to be a straightforward experiment. Both two and three dimensional simulations have been carried out and gave very similar results; unlike the closed box case above, section 7.2. Therefore, since the two dimensional cases were much quicker to run, most of the simulations have been only two dimensional.

Initially the only experimental data available were the pressure histories and there was evidence available that external conditions had a significant effect on peak over pressures, consequently a good deal of attention was paid to boundary conditions. In the simulation it was possible, of course, to consider a box with a specified gas-air mixture open through the vent to a venting region. In the experiment it was necessary to close off the box using cling film in order to fill it with an uniform gas-air mixture. This cling film was left over the end of the box during the explosion. By inspection of the pressure histories it was estimated that the cling film was able to contain pressures of up to 0.1 bar. In a crude attempt to simulate the effect of the cling film the vent model was devised, see section 4.5. This simply allowed for venting when the pressure across the vent reached a critical threshold value. The result of using this can be seen in figure 7. Significant modifications to the early pressure history are obtained but still the peak over pressure is only about 0.1 bar in this simulation. No attempts were made to model the cling film accurately as this would have required a moving grid since the cling film stretches considerably before it breaks.

Further experimental results were soon available after a transparent top was put on the box and high speed cine films were made of the explosions. Subsequently much higher quality high speed video pictures were also obtained. These results allowed the actual flame development to be seen and this could be compared with animations of the flame development in the simulations. An animation of this case has been provided with the software delivered to HSE. The problem can be understood by inspection of figure 8. This shows the vector field coloured by the mass fraction of products at a time when the flame has passed the first baffle and has just reached the location of the second baffle along the centre line of the box. A recirculation region can be seen just behind the first baffle and the flame has bulged out between this recirculation and the next baffle before slimming down

again to pass by the next baffle. In an animation of this simulation it seems that the flame simply compresses the recirculation region but does not penetrate it. By contrast the behaviour of the real flame is quite different. The real flame mushrooms out once it has passed the recirculation region; the edge of the mushroom then passes into the recirculation region itself when the burning becomes very turbulent and fast. This high combustion rate in the recirculation region compresses the gas along the centre of the box and squirts it and the flame past the next baffle where the process is repeated 'a fortiori'. From this it became apparent that the model was failing not because of boundary condition problems but due to the failure of the flame to penetrate the recirculation region.

The progress of the flame into the recirculation region is controlled by turbulent diffusion and so this is where the fault lies. The turbulence model was the one area of physical modelling which had not been changed throughout all of the modelling work done for this project. The reason for this was that turbulence modelling provides infinite scope for 'fitting' results and so it was decided to use only the default K-epsilon model in CFDS-FLOW3D. For in addition to the various turbulence model parameters which can be changed there are many terms which can be included on physical grounds into the model for reacting compressible fluids which are not present in CFDS-FLOW3D, see Jones, W.P., (1979). It was decided in this case to reduce turbulent Prandtl numbers to increase diffusion and this did increase the over pressures, however, the qualitative behaviour of the flame front still did not resemble the experimental results closely.

In gaseous deflagrations hot low density gas accelerates into cold high density gas. This is just the situation where the Rayleigh-Taylor instability should operate and this instability should generate extra turbulence. In the standard turbulence models available in CFDS-FLOW3D terms to represent this instability are not present. A preliminary attempt to include these terms was made at the very end of the project and significant improvements to the qualitative behaviour of the flame front propagation were observed. No time was available to investigate in detail, however, the relevant routines have been delivered to HSE so that investigations may continue there.

It may turn out, however, that the shear layer past the baffles needs to be much better resolved. Grid sensitivity tests have been carried out but no improvement was detected. In order to properly resolve the shear layer perhaps a non-uniform grid should be used with the cells concentrated in the region where the shear layer is generated.

By simply tuning turbulence parameters it may well have been possible to get the 'right answer' for the over pressure, however, the superb video pictures of the experiment leave no room for this kind of tinkering. Because of the good experimental data a great deal of worthwhile work on the modelling of this experiment remains to be done.

#### 7.4 The CCRL furnace case.

The Combustion and Carbonization Research Laboratory (CCRL) of the Canadian Centre for Mineral and Energy Technology (CANMET) made available a large set of experimental data for validating models of coal combustion. This data was used in the Harwell Coal Combustion Programme (HCCP), Stopford, P.J, and Marriott, N. (1990) to validate the coal combustion models in a program called PCOC and these models were subsequently transferred to CFDS-FLOW3D. The CCRL furnace is set up as a standard reference example that comes with the CFDS-FLOW3D software. The furnace is a 5

metre long cylindrically symmetric furnace with a quartz. The simplest coal combustion model uses a one step devolatilisation model identical to that used in the dust explosion model. Unlike the dust explosion model, however, in the standard coal combustion model the coal particles are tracked individually using a Lagrangian method and the radiation field is computed using RAD3D.

A case with 50 micron diameter coal particles was chosen, small enough to ensure that the coal particles would move with the gas so that the dust explosion model would be valid. Very good comparison with CFDS-FLOW3D results was obtained though peak temperatures were rather lower. Interestingly enough the dust explosion model gave better comparison with experiment! The main reason for this was that the coal model was set up with only 32 particles which is too few to give good answers. Also the grid was rather crude. A run of the coal model using a finer grid with many more particles done for the HCCP gave good agreement with experiment. This case, although not relevant to explosion modelling, proved extremely useful in shaking down the explosion software as it exposed several deficiencies in the radiation algorithm which was improved greatly as a result. Final discrepancies in the results were mainly due to the diffusion approximation for radiation transport which was not a good approximation in the quartz region.

#### 7.5 The Peat bomb experiments.

Lars Kjaldman published a paper 'Numerical flow simulation of dust deflagrations' in Powder Technology, 71, (1992). This work detailed the simulation of experiments in which fine powdered peat dust was ignited in a 20 litre spherical steel vessel. In addition it was possible to obtain a much more detailed internal report of this work directly from Kjaldman. The importance of this work is that all the data necessary to perform a simulation were available from the report. This is particularly important as, with the exception of coal dusts burnt by power generators, most of these data are unavailable. In addition to this the initial conditions and ignition were specified.

Kjaldman's simulation results were reasonable qualitative approximations to the experimental results. However, because of the crudeness of the grid and his use of first order differencing schemes plus the uncertainty in certain physical parameters great accuracy could not be expected. He also used somewhat more sophisticated models than are used here, including char combustion and treating the dust as a separate phase so that it could have its own velocity and temperature fields.

Results for the 54 micron, dry dust are shown in figure 9. The peak pressure adjusted for ignition is about 8.8 bar or about 0.4 bar higher than experiment and the time to peak pressure is about 60 ms and the maximum rate of pressure rise is about  $520 \text{ bar s}^{-1}$ . Comparing our results with the experimental results it is clear that the major problem is that the cooling is too low. This is to be expected as the radiation model assumes that the system is optically thick. For this small geometry, however, the optical depth is just less than one and so the radiation diffusion approximation is very poor. In particular the radiative flux at the wall will be under estimated since the radiation temperature at the wall is assumed to equal the wall temperature. Increasing the cooling would clearly reduce the peak over pressure and it would also reduce the timescale because the pressure rise over the last 20 ms is very slow implying that the heat release rate only just exceeds the cooling rate.

In order to get even qualitative agreement it was necessary to modify the gaseous com-

bustion model. The burning rate had to be made independent of the product mass fraction, implying the absence of any localised flame front. This is the same combustion model that Kjaldman used. It implies that where ever gaseous fuel exists it can burn immediately and so the timescales are largely controlled by the rate of devolatilisation. Presumably the presence of hot particles from the igniter, which are spread throughout the volume after 10 ms, causes immediate ignition of gaseous fuel.

A larger scale more realistic experiment would provide a much better test of the software, The results of the 20 litre bomb are, however, as accurate as can be expected and so indicate that no gross errors exist in the implementation.

#### 7.6 Miscellaneous cases.

The Raufoss tube experiment, Moen et al., 1982 has not been revisited again because it is not a suitable case for validation. Even if the geometry were set up so that the ignition could be accurately modelled the external boundary conditions are not correctly known. In addition it has been reported, Hjertager, (private communication), that the end baffle was made from plywood and usually broke during the experiments.

The SOLVEX case has also not been continued with. This is mainly because it is a very large 3 dimensional case and the quasi-laminar phase continues to scales of several metres before the flame reaches the pipes and becomes turbulent. An accurate treatment of the early flame is thus very difficult as self-acceleration is important. Again it may be possible to use the extra turbulence source terms to provide a model for self-acceleration since these extra terms will generate turbulence at the flame front from the Rayleigh-Taylor instability.

## 8 CONCLUSIONS.

### 8.1 Phase three.

The last phase of this project has accomplished the fine tuning of the gaseous explosion models and the dust explosion models have been added and validated. Most importantly the software, which has all been delivered to HSE at Buxton and is in use there, has been provided in a user friendly form with documentation. In addition to the modelling software itself a special set of visualisation software has been provided as well as the standard post-processing software package to enable full three dimensional animations to be produced. The complete software package provided to HSE is competitive with any other explosion modelling software on the market for its defined area of applicability, including such packages as EXSIM which are the result of international collaboration. The same software may also be used for many other areas of interest to HSE, such as the dispersion of heavy gases, fire modelling, ventilation and jet & pool fires.

The results of the simulations in comparison with experiment are generally good though the vented box experiment conducted at HSE is an exception. The software is quite modular from the point of view of the special explosion modelling and so further development of these models at HSE is feasible if required.

## 8.2 The explosion modelling project.

This project has met nearly all the goals set for it with the exception, perhaps, of the ideal of providing a black box explosion prediction facility. Software has been developed for modelling both gas and dust explosions in uncongested regions which can be used by anyone familiar with the CFDS ENVIRONMENT suite of software. Because of this it can be used as an every day tool for investigating explosions. In addition the modularity of the programming used to include the explosion physics allows for easy further development of these models. Simple plots of pressure histories are insufficient to provide an in depth understanding of what is going on and so advanced visualisation tools have been provided to enable both static and animated three dimensional graphics.

The modelling was restricted to open geometries, that is systems which can be completely resolved geometrically. This restriction does impose a limit to the geometrical complexity of a model, due to the finiteness of computer resources. However, it also removes the need for complicated models of sub-grid scale phenomena. Indeed it should be noted that a prerequisite for any serious attempt at modelling congested regions is a good model for open regions. This is because the correlations needed for flame propagation in a congested region depend on knowing the behaviour of the flame around the objects which are not resolved.

For interpolation the software provides a reliable tool for explosion prediction. This is not unreasonably restrictive for small scale explosions where experimental data are not too expensive to obtain. When attempting to simulate a completely new geometrical configuration or a geometry with a quite different scale care is needed. In particular if the system is vented so that the evolution of the flame front depends critically on the behaviour of the flow around a particular object then great care is required before accepting the results. For most systems though the results are quite reliable and the simulations provide a very useful means for investigating the details of what occurs.

## 8.3 Possible future developments.

Before the software is ready for use by untrained practitioners who are interested in engineering fire proof apparatus, for example, a good deal of further development is still needed. It is clear, from this report, that the models used still have plenty of room for improvement. In particular extra physical effects could be included in the turbulence models and also no account has yet been taken of the enhanced quenching near to walls. For such models to be included detailed validation is needed of the sort that can only be obtained by doing high quality experiments in relatively simple geometries of the sort already performed at HSE on the baffled box.

The Leeds linked vessels experiments indicated short comings in the models at the extreme flow speeds and turbulent intensities found there. More sophisticated quenching models which take into account the temperature and pressure of the unburnt gas are needed here, perhaps through including these explicitly in the laminar flame speed. Validation could be provided by using any closed system which generates flames speeds close to the speed of sound or by using the results already obtained at Leeds.

The dust explosion model is still at quite an early stage of development and would benefit greatly from a large scale validation experiment. Scales of metres, or tens of metres ideally, are needed before the model is well within its region of validity. The dust should be stirred up before ignition and flame speed and pressure measurements should be made. The dust needs to be as homogeneous as possible in all of its properties and measurements will need to be available to determine the devolatilisation parameters. The most likely candidate would be a coal dust of the type used for combustion experiments. As soon as such an experiment has been conducted data would be available which would justify further development of the models, for example the lifting of dust off surfaces, particle coalescence etc.

## 9 REFERENCES.

- 1 Allsop, J.A. and Eaton, G.E., Experimental validation of methods for predicting explosion pressures in confined spaces: Summary of results obtained for a flameproof enclosure, HSE Internal Report, IR/L/GE/94/01, 1994.
- 2 Bakke, J.R., Numerical simulation of gas explosions in two dimensional geometries, Christian Michelsen Institute, CMI 865403-8, 1986.
- 3 Bradley, D., Lau, A.K.C. and Lawes, M, Flame stretch rate as a determinant of turbulent burning velocity, Phil. Trans. R. Soc. Lond., A, **338**, 359, 1992.
- 4 Bradley, D., Chen, Z. and Swithenbank, J.R., Burning rates in turbulent fine dust-air explosions, 22nd Symp. (Int.) on Comb./The Combustion Institute, 1767-1775, 1988.
- 5 Freeman, D.J., Experimental validation of methods for predicting explosion pressures in confined spaces: Summary of results obtained for a baffled, vented enclosure, HSE Internal Report IR/L/GE/94/03.
- 6 FLOW3D Manuals, Computational Fluid Dynamics Services, AEA Technology, 1992.
- 7 Kjälman, L., Numerical flow simulation of dust deflagrations, Powder Technology, **71**, 1992.
- 8 Hjertager, B.H., Simulation of transient compressible reactive flows, Comb Sci. and Tech., **27**, 159, 1982.
- 9 Jones, W.P. Models for turbulent flows with variable density and combustion, Von Karman Inst. Book Lecture Series, pp379-421, 1979.
- 10 Moen, I.O., Lee, J.H.S., Hjertager, B.H., Eckhoff, R.K., Pressure Development Due to Turbulent Flame Propagation in Large-Scale Methane-air Explosions, Combustion and Flame, **47**, 31, 1982.
- 11 Phylaktou, K. and Andrews, G.E., Gas explosions in linked vessels, J. Loss Prev. Process Ind., **6**, No. 1, 15, 1993.
- 12 Pope, S.B., PDF methods for turbulent reactive flows, Prog. Energy Comb. Sci. **11**, 119, 1985.
- 13 Stopford, P.J. and Marriott, N., in "Seminar on the Harwell Coal Combustion Programme", pp 59-75, 1990, ed. Sykes, J.

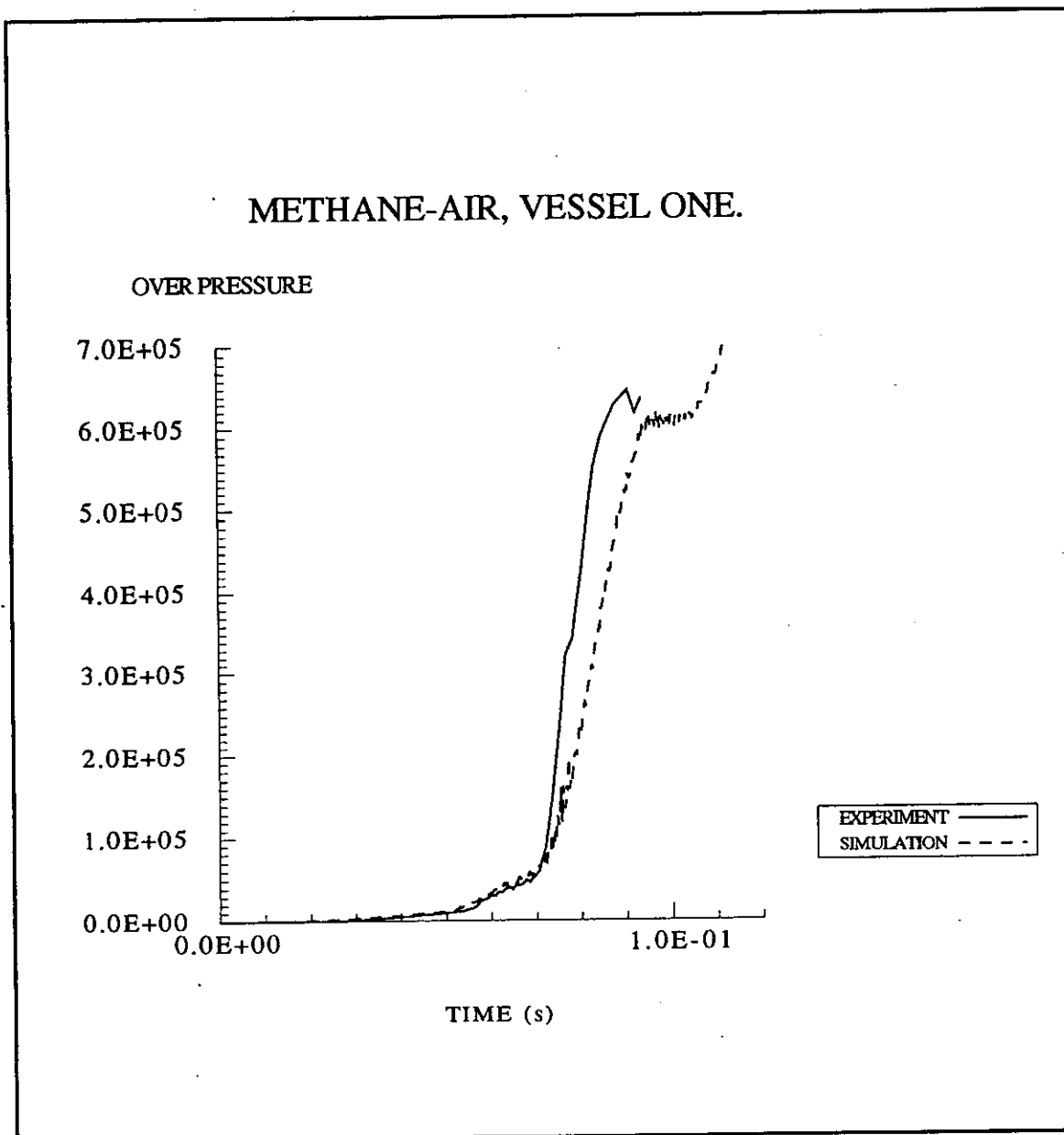


Figure 1.

This figure shows the comparison between experiment and simulation for the pressure history in the Leeds Linked vessels experiment with methane and air. The ignition is central in vessel 1. The comparison is for vessel 1.

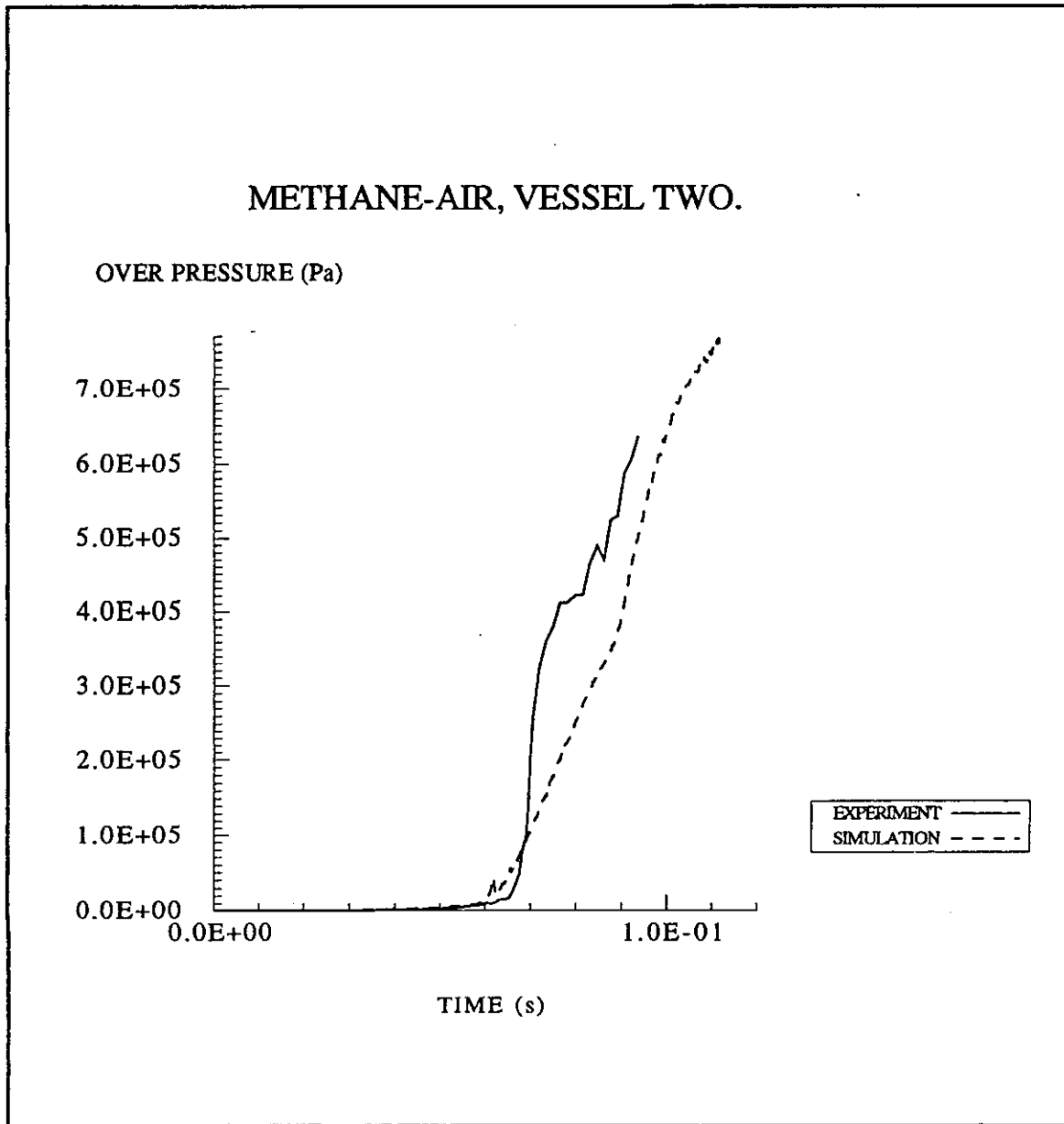


Figure 2.

This is the same as figure 1 except that the comparison is for vessel 2.

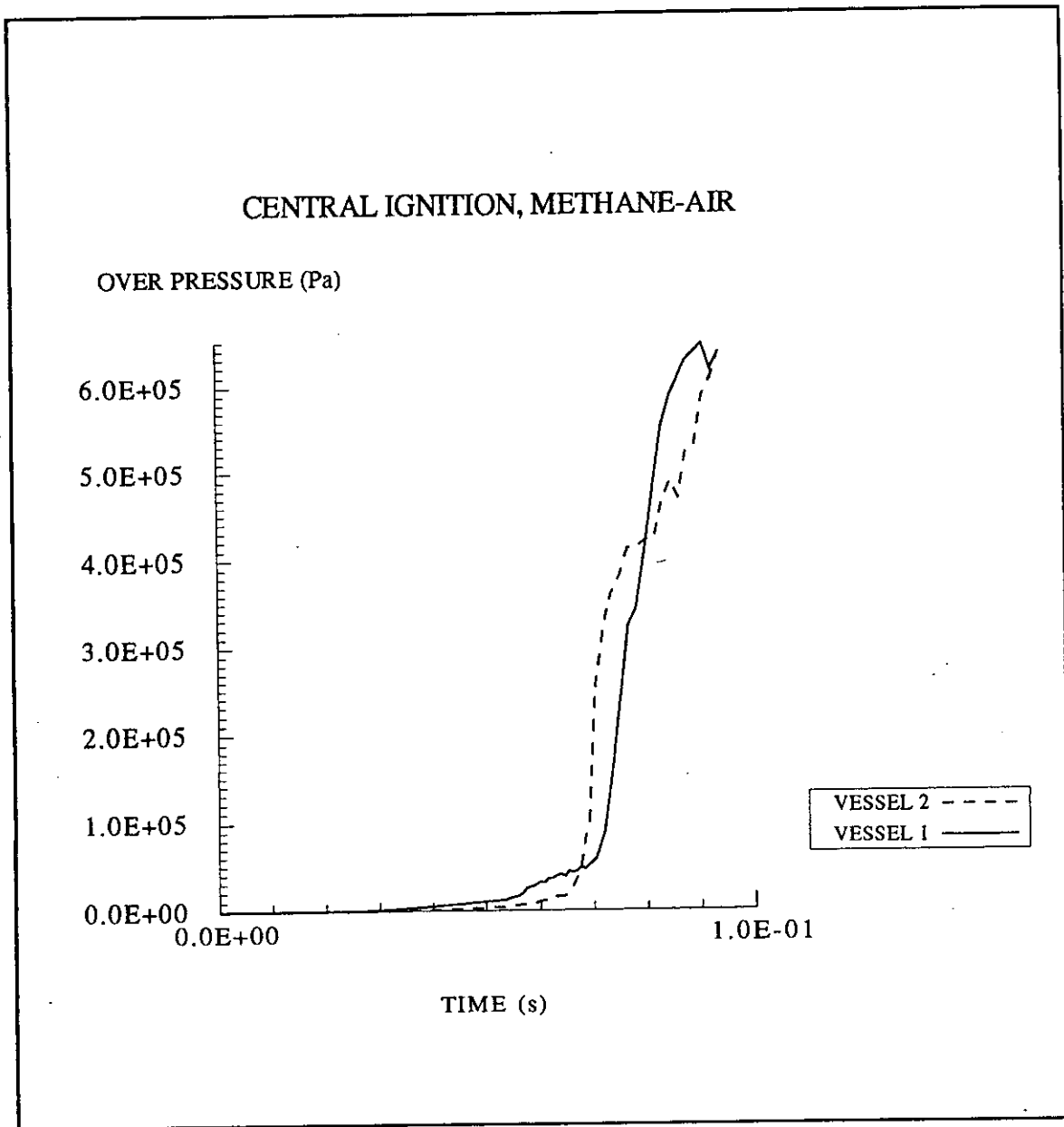


Figure 3.

This figure shows the pressure histories for vessels 1 and 2 for the experimental results for centrally ignited methane and air.

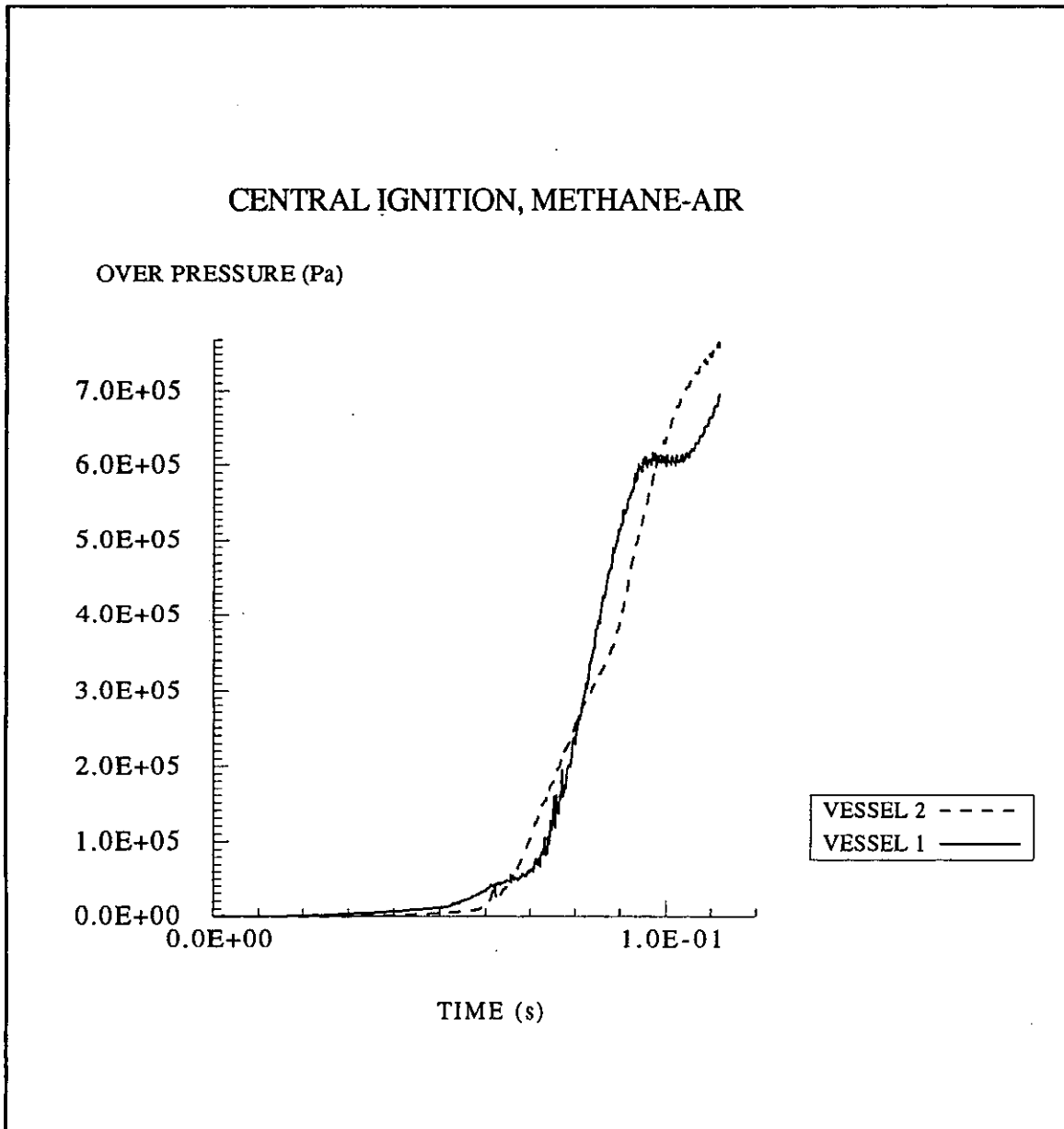


Figure 4.

This shows the pressure histories for the simulation of the centrally ignited methane air mixture in the two vessels.

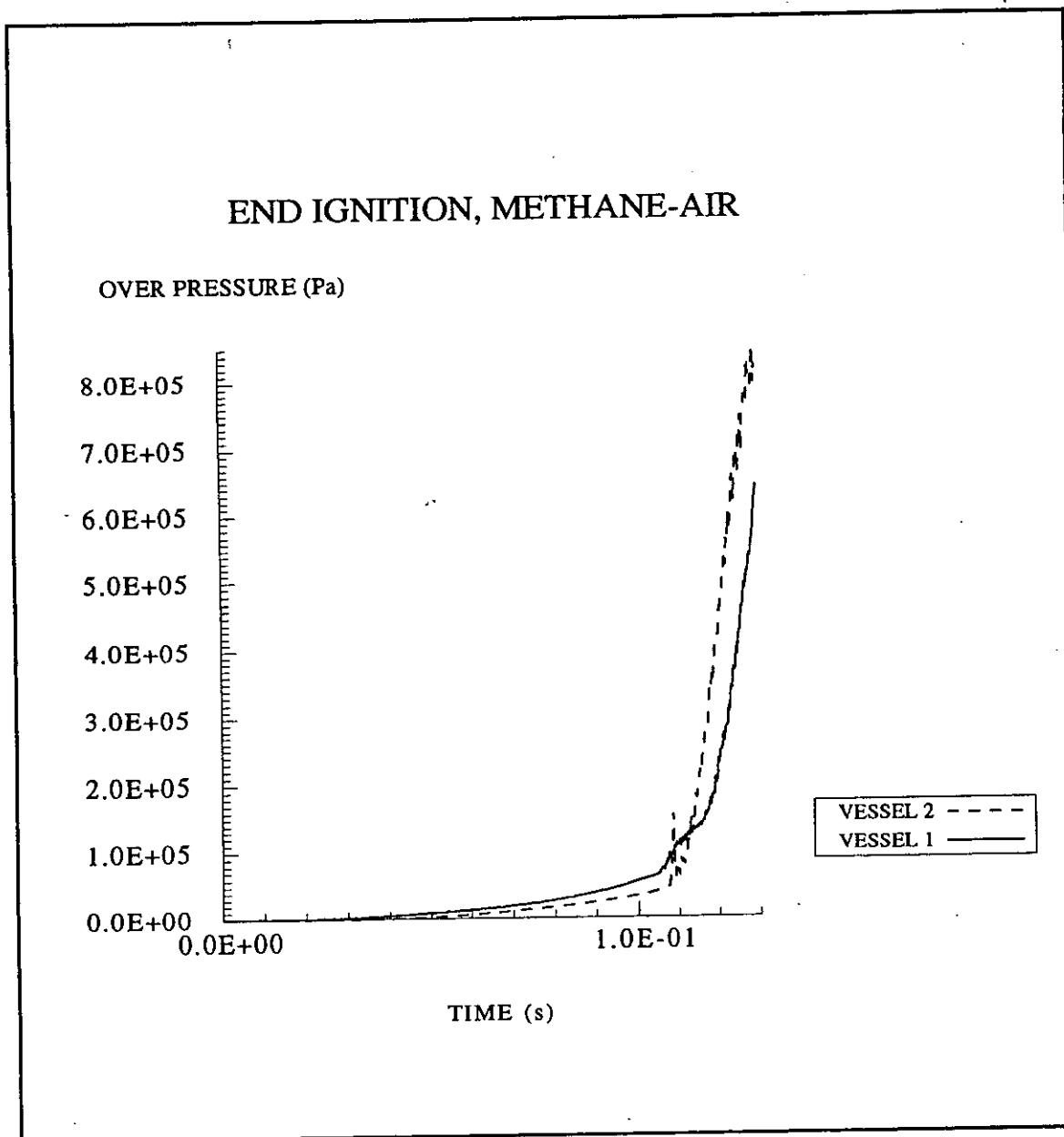


Figure 5.

This figure shows the pressure histories for a simulation of the linked vessels case with end ignition.

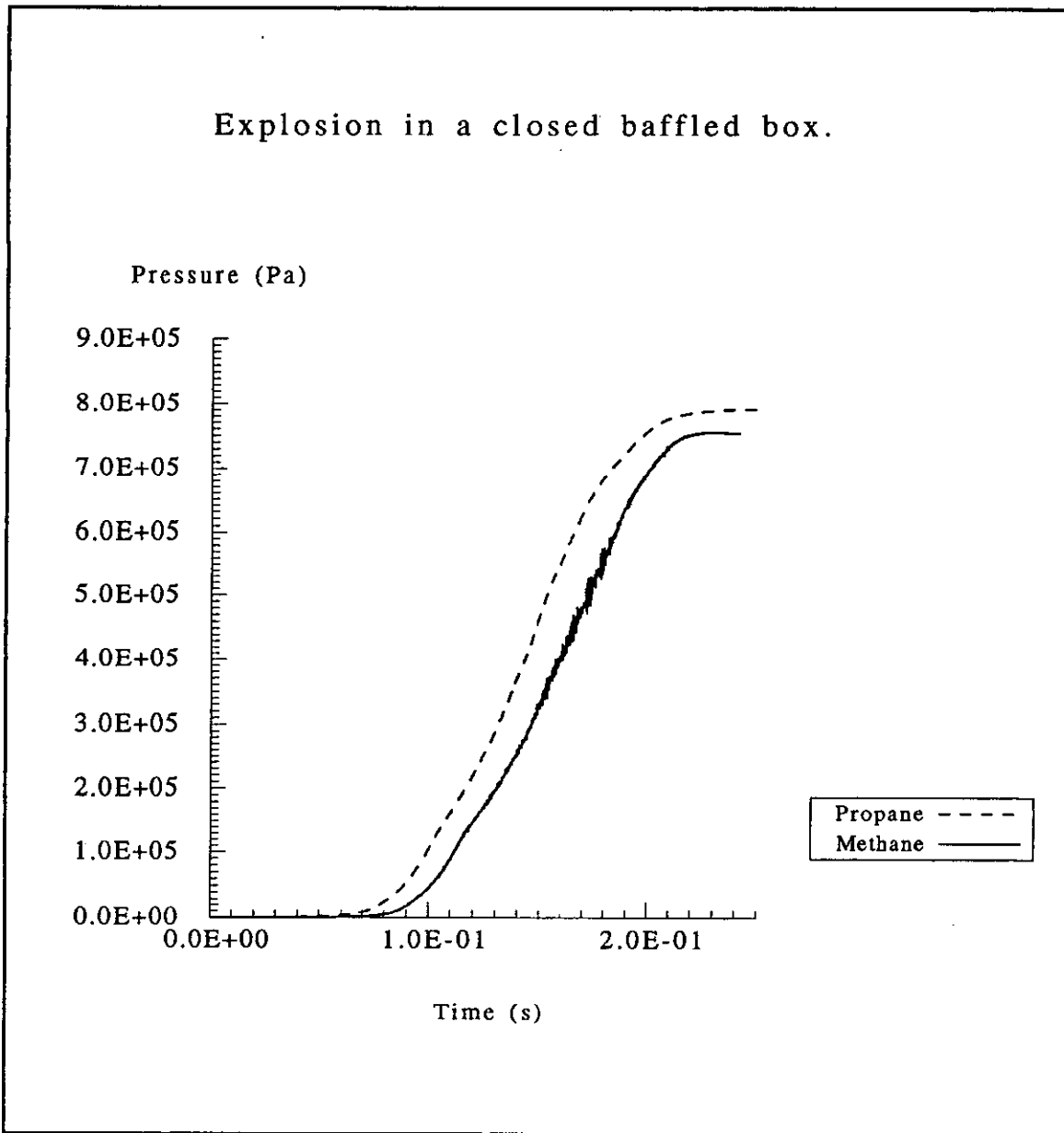


Figure 6.

This figure shows the pressure history for the three dimensional simulation of a 4.3% propane-air and 10% methane-air mixtures in the baffled box enclosure with six baffles. It was centrally ignited between the base plate and the box wall. The walls were modelled as isothermal.

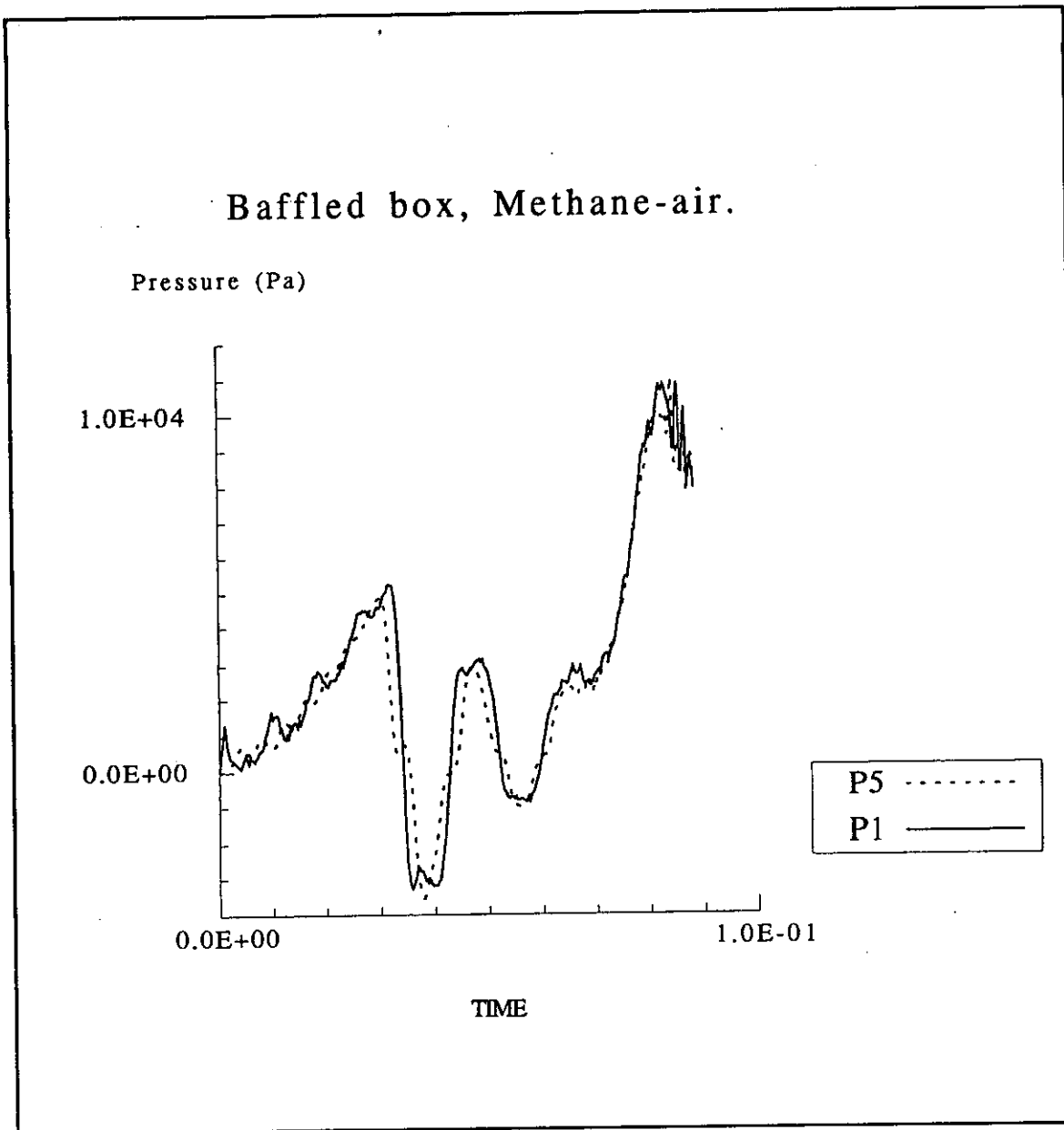


Figure 7.

Methane-air mixture in 5-baffle box. Pressure histories at points P1 and P5 as specified in HSE project report IR/L/FR/93/18, IR/L/GE/93/14 by C.J. Lea and D.J. Freeman.

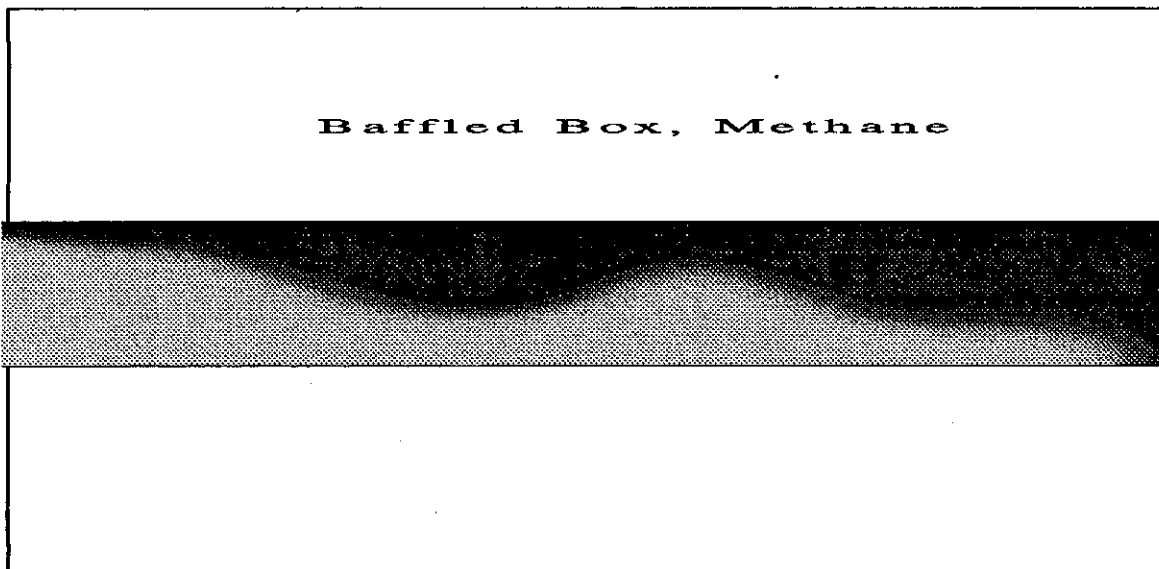


Figure 8a.

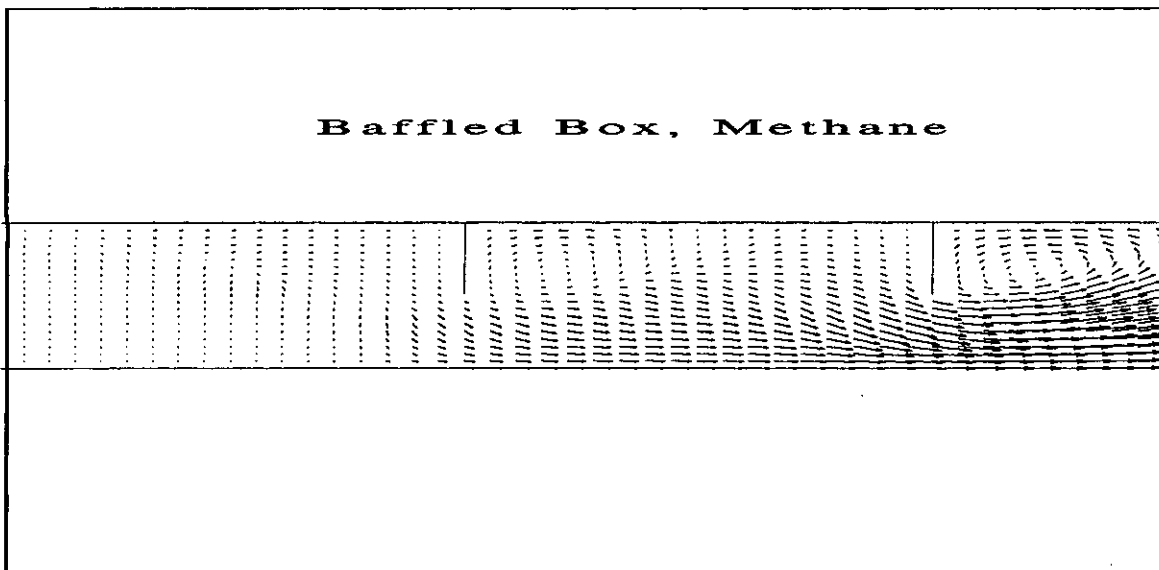


Figure 8b.

These figures show the mass fraction of products and the velocity field at the time when the flame front is just passing by the second baffle, in the baffled box simulation with no venting. It can be seen that the flame has not penetrated the recirculation region behind the first baffle in contrast to the results shown by the high speed video from the experiment.

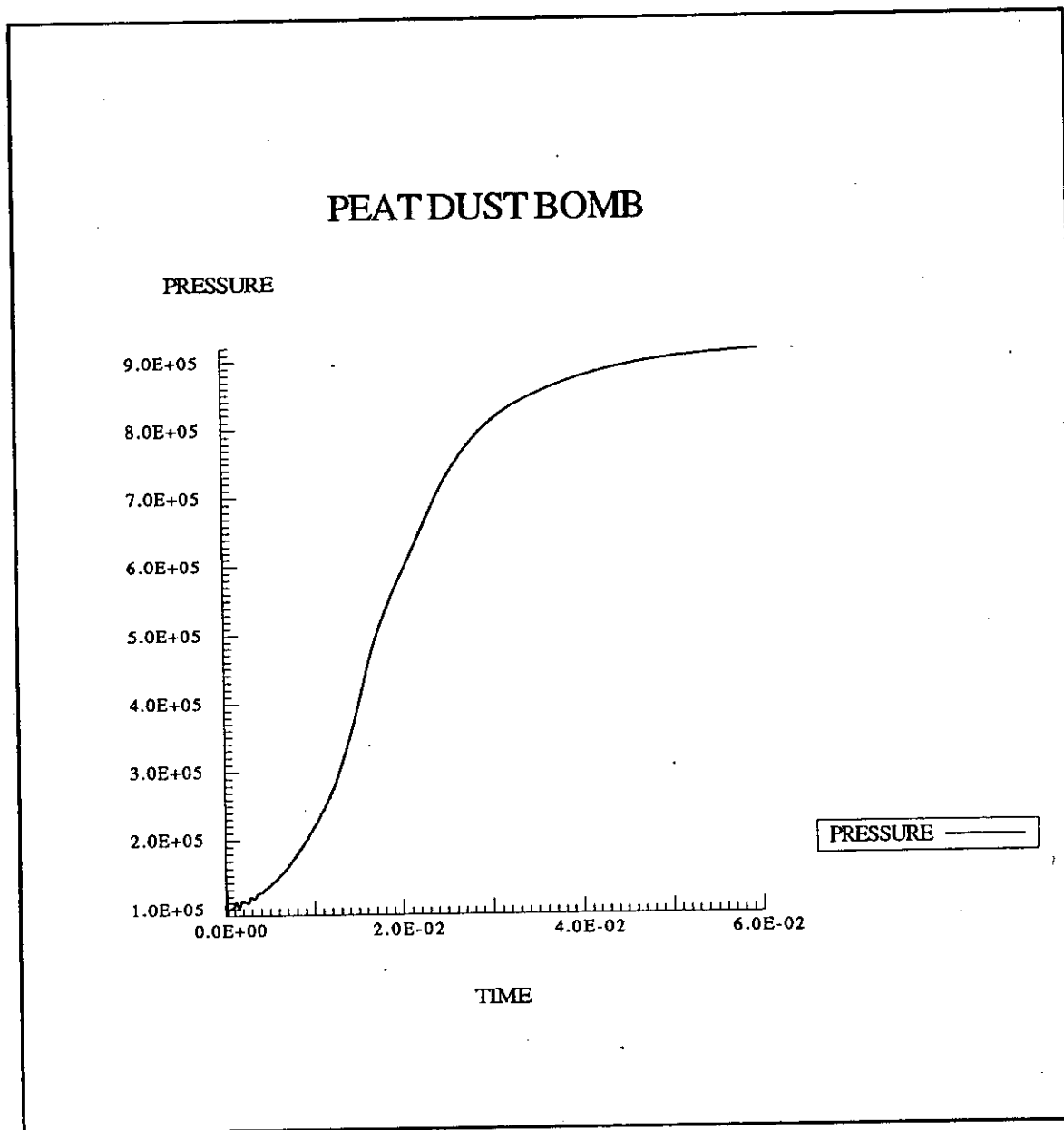


Figure 9.

This figure shows the pressure-time history for 54 micron dry dust. The pressure rise due to the emission of heat and mass by the ignitors has not been subtracted and amounts to approximately 0.4 bar.

## Appendix 1

### The Ignition Model.

This appendix describes the simple ignition model used to simulate point ignition. The modifications necessary to deal with line and plane ignition are straightforward. The maximum spatial resolution that can be achieved numerically is determined by the grid used to discretise the fluid equations. Clearly for point ignition the size of the combustion region will be on a sub-grid scale initially and so this phase must be modelled.

The flame is assumed to be spherical and burn at the laminar rate. Then conservation of mass implies

$$R^2 \rho_c S_b = R^2 \rho_h S_f. \quad (\text{A1.1})$$

Where  $R$  is the flame radius;  $\rho_c$  is the density of the cold pre-combustion gas;  $\rho_h$  is the density of the hot post-combustion gas;  $S_b$  is the burning speed and  $S_f$  is the flame front speed. The flame front speed is thus

$$S_f = \frac{\rho_c}{\rho_h} S_b. \quad (\text{A1.2})$$

The heat released by the flame front is

$$\begin{aligned} \dot{H} &= 4\pi S_f^2 t^2 \rho_c S_b m_f H_f \\ &= 4\pi \rho_h R_i^3 H_f \frac{m_f}{t_i} \left(\frac{t}{t_i}\right)^2 \quad ; \quad t_i \equiv \frac{R_i}{S_f}. \end{aligned} \quad (\text{A1.3})$$

$m_f$  is the mass fraction of fuel, assumed lean or stoichiometric;  $H_f$  is the heat of fuel and  $R_i$  is the radius of the modelled ignition region, typically a few cells across. The burning speed has been assumed to be constant; a good approximation provided that  $R_i$  is not too large.

For numerical reasons it is assumed that the heat is released uniformly across the ignition region. It is also necessary to relate the heat release to the mean rate of change of the fuel mass fraction in the ignition region so that the total energy of the system, chemical plus thermal energy is conserved. Now

$$\dot{H} = \dot{m}_f H_f \bar{\rho} \frac{4\pi}{3} R_i^3. \quad (\text{A1.4})$$

Using equations A1.3 and A1.4 one obtains

$$\dot{m}_f = -\frac{3\rho_h}{\bar{\rho}} \frac{m_f}{t_i} \left(\frac{t}{t_i}\right)^2 \quad (\text{A1.5})$$

where the mean density in the ignition region is

$$\bar{\rho} = \rho_h \left(\frac{t}{t_i}\right)^3 + \rho_c \left(1 - \left(\frac{t}{t_i}\right)^3\right). \quad (\text{A1.6})$$

The actual geometry of the modelled ignition region is not exactly spherical and most of the heat is released at  $t = t_i$ . Therefore, a simplified fuel mass fraction source term is used:

$$\dot{m}_f = \begin{cases} -\frac{m_f}{t_i} \left(\frac{t}{t_i}\right)^2 & \text{for } t \leq t_i \\ 0 & \text{for } t > t_i \end{cases}. \quad (\text{A1.7})$$

This form does not give a smooth transition to the quasi-laminar phase but ensures that the timescale for ignition is accurate.

## Appendix 2

### The thin flame model.

During the early post-ignition phase of flame growth the flame front is thin, that is, its physical width is smaller than the grid spacing. Initially the flame front is laminar and very thin, however, even when the flame front is significantly modified by turbulence it can still be much thinner than the grid spacing. The simulated width of the flame cannot be less than one grid cell wide and so it is necessary to model the heat release. Let the combustion process be characterised by a progress variable  $\phi$ , where  $0 < \phi < 1$ , where  $\phi = 1$  implies unburnt gas. Consider a set of values  $\phi_i$  along a line normal to the flame front located at points separated by distances  $\Delta_i$  and which move with the gas. The model equation for the progress variable is then:

$$\frac{d\phi_i}{dt} = - \begin{cases} \frac{\phi_i}{t_B} & \text{for } \phi_{i-1} \leq \alpha \\ 0 & \text{for } \phi_{i-1} > \alpha \end{cases}; \quad (\text{A2.1})$$

$\alpha$  is a constant,  $0 < \alpha < 1$ , and  $t_B$  is the burning time. The burning speed is

$$S_B = \frac{\Delta_i}{t_B \log \frac{1}{\alpha}}. \quad (\text{A2.2})$$

If the burning speed is known and  $\alpha$  has been chosen then  $t_B$  can be found from equation A2.2 and the evolution of the progress variable found from A2.1.  $\alpha$  determines the width of the modelled flame since burning only takes place in a cell when the previous cell has burnt sufficiently for  $\phi$  to be smaller than  $\alpha$ . Since the real flame front thickness is less than the grid spacing for this model to be used  $\alpha$  should not be too large as the model flame front will then be spread over several cells. On the other hand if  $\alpha$  is too small the flame front only occupies one cell and the burning rate is very large when a cell begins to burn causing large perturbations to the solution with a wavelength of one grid cell. This is undesirable and so some moderate value of  $\alpha$  is used.

For a laminar flame the burning speed is a function of the gas composition and the temperature and pressure. A good deal of data is available for the flame speed in this phase, however, even small amounts of turbulence affect flame propagation and this must be modelled. The burning velocity correlations derived by Bradley, Lau & Lawes (1992), are used. The relations used in the model are only minor modifications of these correlations, however, they are presented here for convenience and completeness.

The burning speed is

$$S_B = S_L + 0.88FK^{-0.3}\sqrt{2k}. \quad (\text{A2.3})$$

$S_L$  is the laminar burning speed;  $F$  is a fitting factor, a value of 2 is used;  $K$  is the Karlovitz stretch factor and  $k$  is the turbulent kinetic energy per unit mass. The Karlovitz stretch factor is given by

$$K = 0.157 \frac{2k}{S_L^2} \left( \frac{\mu_L}{\mu_T} \right)^{0.5}. \quad (\text{A2.4})$$

$\mu_L$  is the laminar dynamic viscosity and  $\mu_T$  is the turbulent dynamic viscosity.

The thin model is used where ever the burning rate computed using the model is greater than the Eddy Break Up (EBU) rate. The thin flame model is, therefore, not simply a precursor to the EBU calculation but is in use throughout the modelling and ensures that all low turbulence regions burn correctly. The laminar flame speed is computed using a 3 point parabolic fit in terms of the equivalence ratio, following the method used by Bakke, (1986):

$$\frac{S_L}{S_{L_{\max}}} = \frac{(x - x_1)(x - x_r)}{(1 - x_1)(1 - x_r)} \quad ; \quad x \equiv \frac{\phi}{\phi_m}. \quad (\text{A2.5})$$

Where  $\phi$  is the equivalence ratio;  $\phi_m$  is the equivalence ratio giving the maximum laminar flame speed;  $S_{L_{\max}}$  is the maximum laminar flame speed and  $x_1$  and  $x_r$  are the lean and rich limits to flame propagation respectively.

In two and three dimensional calculations the cell ignition criterion is applied by inspecting all neighbours of a given cell and burning is assumed to begin if the progress variable in any of them is less than  $\alpha$ . This approximation ignores the direction of motion of the flame and so introduces a significant error if the cell dimensions are comparable to, or larger than, the radius of curvature of the flame front.

## Appendix 3

### The Eddy Break Up combustion model.

The Eddy Break Up (EBU) model used is the standard EBU model available in CFDS-FLOW3D together with an additional ignition criterion. The ignition criterion is based on a product mass fraction threshold and is essential to avoid 'spontaneous' ignition due to numerical effects. The more complex Damköhler cut-off has been abandoned because it conflicts with the quenching model used, see appendix 4. The product mass fraction threshold is equivalent to a temperature threshold and so operates in a similar manner to the Damköhler cut-off.

The combustion rate is determined by the rate of change of the mass fraction of fuel which is given by

$$\frac{\partial}{\partial t}(\rho m_f) + \nabla \cdot (\rho U m_f) - \nabla \cdot \left( \left( \frac{\mu_T}{\sigma_T} + \frac{\mu}{\sigma} \right) \nabla m_f \right) = -\rho \frac{\varepsilon}{k} C_R C_A M_{lim}. \quad (A3.1)$$

$U$  is the flow velocity;  $\sigma$  and  $\sigma_T$  are the laminar and turbulent Prandtl numbers and  $\varepsilon$  is the rate of turbulent energy dissipation. The terms  $C_R$ ,  $C_A$  and  $M_{lim}$  are modelled as:

$$C_R = 23.6 \left( \frac{\mu \varepsilon}{\rho k^2} \right)^{0.25}; \quad (A3.2)$$

$$C_A = \begin{cases} 1.0 & m_p \geq m_{pi}; \\ 0.0 & m_p < m_{pi}; \end{cases} \quad (A3.3)$$

$$M_{lim} = \min \left( m_f, \frac{m_o}{i}, \frac{m_p}{1+i} \right). \quad (A3.4)$$

$m_p$  and  $m_o$  are the mass fractions of products and oxidant respectively;  $m_{pi}$  is the ignition threshold value of products, set to 0.1 for a stoichiometric methane air mixture, and 1:i is the stoichiometric ratio of the fuel to oxidant. There are three unknowns, the three mass fractions, and so two further equations are used to close the set. Firstly the sum of the mass fractions must be unity. Secondly the mixture fraction is a conserved quantity and has its own conservative transport equation, see the CFDS-FLOW3D user manual, 1993. Using the mean mixture fraction,  $F$ , the following relation is obtained

$$m_p = \frac{F - m_f}{F_{st}}. \quad (A3.5)$$

$F_{st}$  is the stoichiometric value of the mixture fraction,  $F$ . Using equations A3.5 and A3.1 it can be seen that if  $M_{lim}$  and  $C_A$  are non-zero and  $\epsilon/k$  is large enough then  $m_p$  will grow exponentially fast. For numerical reasons  $m_p$  will eventually become non-zero everywhere, even far from the combustion region. The non-zero ignition value of  $m_p$  is therefore required to prevent 'spontaneous' combustion occurring in regions of intense turbulence before the flame front reaches them.

## Appendix 4

### Quenching.

It is well known that if a flame is stretched sufficiently extinction will occur. The major difficulty with turbulence induced stretch is in obtaining a quantitatively accurate, general model for quenching. Turbulence induces a wide distribution of strain rates in a flow, a distribution which changes with time. In the absence of a direct numerical flow simulation a proper statistical treatment of the fluid should be used, see e.g. Pope, 1985. For our current work these methods are far too computationally expensive and even the more modest programme of including a fixed probability density function (pdf) for the turbulent fluctuations in the strain rate would need a major software development effort which is probably unjustified. Bradley, Lau & Lawes, 1992, have investigated such pdf's and find that a Gaussian pdf is sufficiently accurate. This implies that quenching will occur exponentially at sufficiently high mean strain rates. The quenching is therefore modelled by:

$$R_f = R_{fu} \exp \left\{ -\frac{D}{D_q} \right\}. \quad (\text{A4.1})$$

$R_f$  and  $R_{fu}$  are the quenched and unquenched fuel consumption rates, respectively.  $D$  is a Damköhler number and  $D_q$  is the quenching threshold. For laminar burning:

$$D = (\epsilon \nu)^{0.5} \frac{1}{S_L^2} \quad (\text{A4.2})$$

where  $\nu$  is the kinematic viscosity. For turbulent burning:

$$D = \frac{\epsilon \nu}{k S_L^2}. \quad (\text{A4.3})$$

The threshold values for the Damköhler numbers are currently set to 10 for laminar quenching and 1 for turbulent quenching.

## Appendix 5

### Dust combustion model.

#### 1 INTRODUCTION.

This appendix describes the dust combustion model in detail. The model is just an extension of the gaseous combustion model as described in appendices 1 to 4. There are two extra mass fractions: a fraction for dust fuel and a fraction for dust inert, or char. In order to describe the evolution of these mass fractions two extra equations are needed and the relationship between the mass fractions and the mixture fraction has to be generalised. Also to describe the transfer of mass between the dust and the gas, devolatilisation, extra source terms are needed in the gas fuel equation, the mixture fraction equation and the enthalpy equation. This modelling of the dust is described in section 2.

The dust contributes nothing to the pressure and is incompressible, therefore it just acts as an extra source of inertia. Essentially the dust particles can be thought of as gigantic molecules with infinite molecular weight for the purposes of the equation of state. This is described in section 3.

Finally radiative heat transport, a process ignored altogether in the gas deflagration model, has to be included. A simple diffusion model for radiation transport is justified and described in section 4.

#### 2 TRANSPORT OF GAS AND DUST FRACTIONS.

The definitions of the mixture fraction and the stoichiometric ratio are unchanged, being defined purely in terms of the gas fractions. The basic combustion equation is:-

$$1 \text{ kg fuel} + i \text{ kg oxidant} = (1 + i) \text{ kg products} . \quad (\text{A5.1})$$

The fuel in equation 1 is just the gaseous fuel, no char combustion is included. The mixture fraction,  $f$ , is given by;

$$f = (1 + im_f - m_o) F_{st} \quad ; \quad F_{st} \equiv \frac{1}{1 + i} . \quad (\text{A5.2})$$

The total mass fraction of dust,  $m_d$ , is the sum of the dust fuel fraction,  $m_{df}$ , and the dust inert fraction,  $m_{di}$ . Using the fact that the mass fractions must sum to unity and equation 2, the mass fraction of products is,

$$m_p = \frac{f - m_f}{F_{st}} - m_d. \quad (\text{A5.3})$$

The fuel mass fraction and the mixture fraction now have the following bounds:-

$$0 \leq m_f \leq f - m_d F_{st} \quad (\text{A5.4})$$

and

$$m_d F_{st} \leq f \leq 1 - i m_d F_{st}. \quad (\text{A5.5})$$

The devolatilisation rate is modelled as a simple single step Arrhenius reaction giving a source term for the gas fuel and dust fuel equations,

$$\left. \frac{\partial}{\partial t} (\rho m_f) \right|_{dv} = \left. \frac{\partial}{\partial t} (\rho m_{df}) \right|_{dv} = \rho m_{df} A e^{-\frac{T_A}{T}} \quad (\text{A5.6})$$

and a source in the mean mixture fraction equation,

$$\left. \frac{\partial}{\partial t} (\rho F) \right|_{dv} = i F_{st} \rho m_{df} A e^{-\frac{T_A}{T}}. \quad (\text{A5.7})$$

The mass fraction of dust inert,  $m_{di}$ , is simply a conservation equation.

### 3 EQUATION OF STATE.

The dust simply contributes to the inertia of the gas as explained in the introduction. The total density is then just the sum of the gas density and the dust density with the gas density being determined by the pressure and temperature through a perfect gas relation as normal:-

$$\rho = \rho_g + \rho_d \Rightarrow \rho = \frac{\rho_g}{1 - m_d}. \quad (\text{A5.8})$$

$\rho$  is the total density;  $\rho_g$  is the gas density and  $\rho_d$  is the dust density. Using the perfect gas law for the gas gives,

$$\rho = \frac{1}{R_g (1 - m_d)} \frac{P}{T_g}. \quad (\text{A5.9})$$

Assuming that the dust is insensitive to the adiabatic temperature changes in a sound wave, the speed of sound is then given by,

$$c_s^2 = \gamma_g \frac{P}{\rho}. \quad (\text{A5.10})$$

#### 4 RADIATION TRANSFER.

Assuming that the particles are large compared to wavelength of the radiation, diameters greater than about 10 microns, then the particle opacity is,

$$k_p = n_p A_{pc}, \quad (\text{A5.11})$$

where  $n_p$  is the particle number density and  $A_{pc}$  is the cross sectional area of a particle. The total emissivity of the particles is,

$$k_p \epsilon_p \frac{A_{ps}}{A_{pc}} \sigma T^4, \quad (\text{A5.12})$$

where  $\epsilon_p$  is the particle emissivity and  $A_{ps}$  is the particle surface area. The effective bulk emissivity is

$$4k_d \sigma T^4, \quad (\text{A5.13})$$

where  $k_d$  is the effective absorption coefficient. Therefore in an optically thick dust,

$$k_d = k_p \epsilon_p \frac{A_{ps}}{4A_{pc}} \quad (\text{A5.14})$$

For spherical particles with a particle density of  $1000 \text{ kgm}^{-3}$  this gives an effective absorption coefficient of:

$$k_d \sim \frac{10^{-3}}{r_p} m_d \epsilon_p. \quad (\text{A5.15})$$

For dust mass loadings of greater than 0.1 systems with dimension of order metres or more will be optically thick for particle sizes of 100 microns or less. For a purely absorbing atmosphere the diffusion approximation gives:

$$\nabla \cdot \left( \frac{1}{k} \nabla J \right) = k \left( J - \frac{\sigma T^4}{\pi} \right), \quad (\text{A5.16})$$

where  $J$  is the mean radiation intensity and  $k$  is the total effective absorption coefficient. The boundary condition at walls is,

$$J = \frac{\sigma T_w^4}{\pi}, \quad (\text{A5.17})$$

where  $T_w$  is the wall temperature.

## Appendix 6

### Three dimensional animations.

A special version of the AVS visualisation package has been customised for HSE so that 3 dimensional animation can be performed. This software is called HSE1VIEW and has been delivered with documentation to HSE at Buxton. hse1view reads in a series of delta files which have been produced by CFDS-FLOW3D. In order to save further on disk space the delta files can be compressed, using the standard unix compress facility, and read in, in their compressed form directly into HSE1VIEW.

The animation output from CFDS-FLOW3D consists of an initial set of variable fields, which are written to the usual dump file in the normal way, and a set of delta files which hold the changes in the variable fields as a function of time. Only grid cells for which the variable has changed by a significant amount since the last time it was written out have deltas written out for them. The algorithm used is as follows:-

Define  $\phi_n(t_i)$  to be the value of the variable at time,  $t_i$ , at cell node n. If the current time is  $t_c$  then the current field value at node n is defined to be:

$$\phi_n^c(t_c) = \sum \delta_n(t_i) + \phi_n(0). \quad (\text{A6.1})$$

The summation is to be taken over all output times up to and including time  $t_c$ . Delta is defined as,

$$\delta_n(t_i) = \phi_n(t_i) - \phi_n^c(t_{i-1}) \quad (\text{A6.2})$$

If a delta were written out every time the field itself was to be output the current field value would be identical to the actual value of the field at every node. The standard deviation of the change in the variable at time  $t_i$  is,

$$\sigma = \sqrt{\frac{1}{N} \sum_n (\delta_n(t_i) - \langle \delta(t_i) \rangle)^2}. \quad (\text{A6.3})$$

A new delta is only written out if:

$$|\delta_n(t_i)| > \alpha \sigma. \quad (\text{A6.4})$$

$\alpha$  is a constant which is set to 0.2. Each delta file written out at specified intervals during a simulation therefore consists of a set of deltas for nodes where the change in the variable obeys inequality 4.



**MAIL ORDER**

HSE priced and free  
publications are  
available from:

HSE Books  
PO Box 1999  
Sudbury  
Suffolk CO10 6FS  
Tel: 01787 881165  
Fax: 01787 313995

**RETAIL**

HSE priced publications  
are available from  
good booksellers.

**PUBLIC ENQUIRY POINT**

Health and safety enquiries:  
HSE Information Centre  
Broad Lane  
Sheffield S3 7HQ  
Tel: 0114 289 2345  
Fax: 0114 289 2333

CRR 93

**£10.00 net**

ISBN 0-7176-1035-7



9 780717 610358